



Reconstructing past upwelling intensity and the seasonal dynamics of primary productivity along the Peruvian coastline from mollusk shell stable isotopes

James Sadler

School of Ocean and Earth Science, National Oceanography Centre, Southampton, University of Southampton Waterfront Campus, European Way, Southampton, SO14 3ZH, UK

Matthieu Carré and Moufok Azzoug

Institut des Sciences de l'Evolution de Montpellier, Université Montpellier 2-CNRS-IRD, CC061, Pl. Eugène Bataillon, F-34095 Montpellier, France (matthieu.carre@univ-montp2.fr)

Andrew J. Schauer

Department of Earth and Space Sciences, University of Washington, Box 351310, Seattle, Washington 98195, USA

Jesus Ledesma

Oceanografía Química, IMARPE, Cruce Esq. Gamarra y Gral Valle s/n Callao, Callao 01, Peru

Fredy Cardenas

Laboratorio Costero de Ilo, IMARPE, Ilo, Callao 01, Peru

Brian M. Chase

Institut des Sciences de l'Evolution de Montpellier, Université Montpellier 2-CNRS-IRD, CC061, Pl. Eugène Bataillon, F-34095 Montpellier, France

Department of Archaeology, History, Culture and Religion, University of Bergen, Postbox 7805, N-5020, Bergen, Norway

Ilhem Bentaleb and Serge D. Muller

Institut des Sciences de l'Evolution de Montpellier, Université Montpellier 2-CNRS-IRD, CC061, Pl. Eugène Bataillon, F-34095 Montpellier, France

Magloire Mandeng

IPSL/OCEAN, UPMC/CNRS/IRD/MNHN, Centre IRD France Nord, 32 ave. Henri Varagnat, F-93143 Bondy CEDEX, France

Eelco J. Rohling

School of Ocean and Earth Science, National Oceanography Centre, Southampton, University of Southampton Waterfront Campus, European Way, Southampton, SO14 3ZH, UK

Julian P. Sachs

School of Oceanography, University of Washington, Box 355351, Seattle, Washington 98195, USA

[1] We present here a potential new method to evaluate past variations of the mean intensity of Peruvian coastal upwelling and of the seasonal timing of phytoplankton blooms. This method uses a combination of the monthly carbon and oxygen isotopic signals preserved in fossil mollusk shells, and a series of corrections

to extract the variations of the dissolved inorganic carbon (DIC) $\delta^{13}\text{C}$. Based on the analysis of five shell samples (85 shells in total) from the southern Peruvian coast, we suggest that the mean coastal upwelling intensity can be determined from a linear relationship between average values of corrected shell $\delta^{13}\text{C}$ and $\delta^{18}\text{O}$. This new potential proxy would bring additional independent information valuable to interpret paleoproductivity changes reconstructed from marine sediment of the nearby continental shelf. Results obtained on fossil samples from the middle Holocene show an increase in upwelling intensity during this period associated to a spatial reorganization of upwelling centers along the South Peruvian coast. At the seasonal scale, corrected shell $\delta^{13}\text{C}$ enrichment indicates a phytoplankton bloom. Seasonal timing of phytoplankton blooms can be estimated by the lag with the annual temperature cycle reproduced by shell $\delta^{18}\text{O}$ monthly variations. The results obtained with two modern shell samples indicate phytoplankton blooms occurring during summer and fall, consistently with in situ productivity observations. Our method relies on revisited assumptions about the influence of temperature and metabolism in mollusk shell $\delta^{13}\text{C}$. We further discussed the validity of these assumptions and the potential implications for the interpretation of similar data sets.

Components: 10,900 words, 8 figures, 3 tables.

Keywords: Peru; marine productivity; mollusk; sclerochronology; stable isotopes; upwelling.

Index Terms: 4924 Paleooceanography: Geochemical tracers; 4964 Paleooceanography: Upwelling (4279).

Received 1 March 2011; **Revised** 23 November 2011; **Accepted** 2 December 2011; **Published** 27 January 2012.

Sadler, J., et al. (2012), Reconstructing past upwelling intensity and the seasonal dynamics of primary productivity along the Peruvian coastline from mollusk shell stable isotopes, *Geochem. Geophys. Geosyst.*, 13, Q01015, doi:10.1029/2011GC003595.

1. Introduction

[2] Marine phytoplankton performs approximately 50% of the net global carbon fixation through photosynthesis, and thus acts as a critical link between the organic and inorganic carbon reservoirs [Behrenfeld *et al.*, 2006; Alvain *et al.*, 2008]. This biological carbon fixation is strongly influenced by climate change in the low latitude oceans, with warmer waters increasing stratification and reducing productivity [Cox *et al.*, 2000; Bopp *et al.*, 2001; Behrenfeld *et al.*, 2006; Steinacher *et al.*, 2010]. The majority of marine primary productivity in the tropics is concentrated in upwelling zones where it is promoted through a supply of nutrients. Upwelling intensity is a major but complex parameter within the global carbon cycle. Deep waters saturated in CO_2 are upwelled and act as a carbon source upon exchange with the atmosphere, while the high primary productivity increases the oceanic biological carbon pump. The response of primary productivity to the rate of upwelling may also be limited by alternate parameters such as terrestrial iron input [Martin *et al.*, 1994; Hutchins *et al.*, 2002; Dezileau *et al.*, 2004] or light availability [Cole and Cloern, 1984]. A comparison of 30 model simulations against in situ data from the tropical Pacific by Friedrichs *et al.* [2009] revealed that the majority

of models significantly underestimate current primary productivity. Estimates of the response of upwelling intensity and marine productivity to greenhouse warming remain highly uncertain.

[3] Reconstructions of past changes in upwelling intensity and marine productivity are required to fully understand their controls and to constrain model simulations. Many studies using marine sediment cores have been devoted to this issue. Despite their high interest, these studies often face two limitations: (1) paleoupwelling intensity are often inferred from paleoproductivity indicators based on the assumption that upwelling systematically promotes productivity, which is not the case in high nutrient low chlorophyll (HNLC) zones such as the Peruvian upwelling and (2) the mean annual carbon export budget simulated in biogeochemical models is an integration of seasonal scale processes that cannot be studied in sediment cores as a result of their low temporal resolution. Seasonal variability in the coastal Peruvian upwelling is recorded in mollusk shell $\Delta^{14}\text{C}$ signals [Jones *et al.*, 2009]. For ancient periods, variations of mean paleoupwelling intensity can be indicated by variations of marine reservoir age estimated by the radiocarbon analysis of contemporaneous marine shells and plant remains [Fontugne *et al.*, 2004; Ortlieb *et al.*, 2011]. However, this method has significant uncertainties

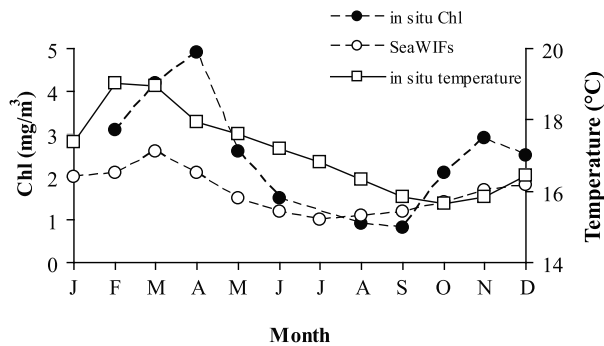


Figure 1. Monthly averages of chlorophyll *a* concentration along the Peruvian coastline from 1997 to 2005. Closed and open circles indicate IMARPE in situ and SeaWiFS surface chlorophyll *a* data respectively, averaged from the 250 km wide coastal zone between 4 and 15°S. The highest chlorophyll *a* concentrations were consistently observed during February, March and April, i.e., austral summer. Modified from the work of *Echevin et al.* [2008]. Monthly sea surface temperature were averaged for the 1925–2002 period from IMARPE in situ measurements in Puerto Chicama, Peru.

because of potential old wood effect and intrashell variability of reservoir age [*Jones et al.*, 2007, 2010]. We propose here to use an alternative paleoenvironmental archive that would yield independent estimates of the coastal upwelling intensity and insights into seasonal scale productivity processes.

[4] The potential of oxygen and carbon stable isotopes in mollusk shells as high resolution paleoupwelling archives has been recognized [*Killingley and Berger*, 1979; *Krantz et al.*, 1987, 1988; *Jones and Allmon*, 1995], yet remains poorly exploited, primarily because of the multiple influences involved in mollusk $\delta^{13}\text{C}$. Here we propose a method combining oxygen and carbon stable isotope records ($\delta^{18}\text{O}$ and $\delta^{13}\text{C}$ respectively) in shells of the mollusk *Mesodesma donacium* resolved to monthly time-scales to study the past variability of (1) the average coastal upwelling rate, and (2) the seasonal timing of coastal phytoplankton blooms, along the coast of Peru. We then applied the method to two fossil shell samples from the middle Holocene and the Inca period for a comparison against modern conditions.

1.1. Coastal Peru

[5] Coastal Peru is characterized by year-round southeasterly trade winds that generate strong Ekman transport and coastal upwelling [*Brink et al.*, 1983; *Huyer et al.*, 1987]. Because the continental slope is so close to the shore in Peru, the surface conditions over the Peruvian shelf are closely related to the coastal upwelling [*Strub et al.*, 1998]. Deep

waters are upwelled along the Peruvian coast in localized upwelling centers and then advected offshore. Therefore, a steep sea-surface temperature (SST) gradient is observed between cool coastal waters and relatively warmer waters offshore. Deep waters are upwelled throughout the year along the Peruvian coastline, with a maximum experienced during the austral winter (June to September).

[6] The vertical advection of deep water provides an annual supply of nutrients to the surface, supporting a highly productive phytoplankton bloom [*Echevin et al.*, 2008; *Taylor et al.*, 2008]. Average chlorophyll *a* concentrations decrease seaward from $\sim 10 \text{ mg/m}^3$ on the coast to $\sim 1 \text{ mg/m}^3$ $\sim 300 \text{ km}$ offshore [*Echevin et al.*, 2008]. Estimates of the paleoenvironmental conditions in this region are largely based on proxies derived from phytoplankton preserved within sediment cores from the continental shelf, approximately 30 to 140 km offshore, within the close influence of the coastal upwelling [*Mohtadi et al.*, 2005]. Whereas low frequency temporal variability ($\geq 10^1 \text{ yr}$) of average productivity is expected to be similar on the coastline and over the shelf, coastal and shelf phytoplankton blooms are characterized by different assemblages with different seasonal timings and strength [*González et al.*, 2004; *Ochoa et al.*, 2010]. Therefore the environmental conditions of the coastline recorded by mollusk shells may be significantly different, at the seasonal scale, from the conditions over the shelf recorded by sediment cores.

[7] Satellite data, in situ sampling and model simulations indicate that blooms along the Peruvian coastline currently occur during austral summer (Figure 1), in opposition to the seasonal phasing of upwelling intensity [*Thomas et al.*, 1994; *Chávez et al.*, 2008; *Echevin et al.*, 2008]. Therefore, unlike the physically analogous Chilean region of the Humboldt Current [*González et al.*, 2004], phytoplankton growth in the coastal Peruvian upwelling is not limited by the nutrient supply from the deep sea, but potentially by light (low stratus cloud cover is persistent from June to November) or the supply of bio-available iron such as observed in the HNLC equatorial Pacific [*Coale et al.*, 1996].

1.2. Environmental Information Potentially Reconstructed From Mollusk Stable Isotopes

[8] High resolution microsampling of *M. donacium* shells (see section 3.1) allows the evaluation of monthly variations in both $\delta^{13}\text{C}$ and $\delta^{18}\text{O}$ incorporated in shell aragonite (CaCO_3). The oxygen isotopic fractionation between aragonite and sea-

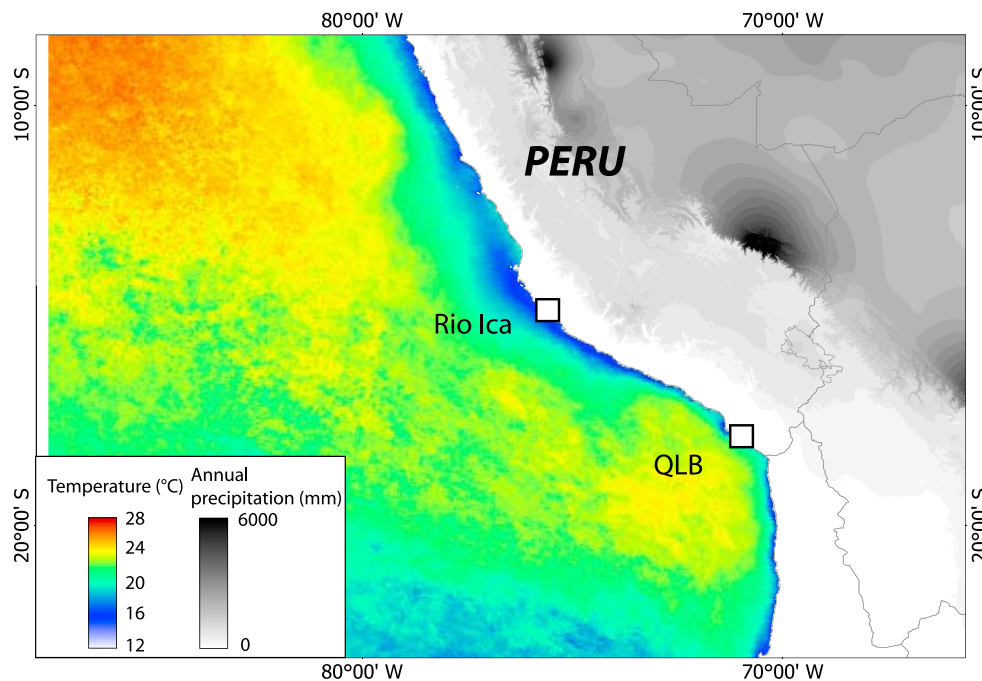


Figure 2. The two sampling sites of Rio Ica and QLB in Southern Peru where both modern and fossil *M. donacium* shells were collected. Greyscale patterns over the continent indicate annual precipitation (Worldclim 1.4 data set). Color patterns in the ocean indicate mean annual sea surface temperature (NASA's MODIS data set). Cooler SSTs along the coast are related to the presence of upwelling, which appears stronger at 15°S near the Ica site than at 18°S near the QLB site.

water is a temperature dependent reaction; therefore the $\delta^{18}\text{O}$ signal from *M. donacium* provides a proxy record for temperature reconstructions provided the seawater $\delta^{18}\text{O}$ can be estimated [Carré *et al.*, 2005a].

[9] The carbon isotopic composition of mollusk shells may have multiple influences: (1) the isotopic composition of the dissolved inorganic carbon (DIC), $\delta^{13}\text{C}_{\text{DIC}}$, (2) the proportion of metabolic carbon in carbonate ions involved in the aragonite precipitation (metabolic effect) (see discussion in section 4.2), (3) kinetic disequilibrium effect (see McConnaughey and Gillikin [2008] for a detailed review) and (4) a temperature-related fractionation for which the mechanisms remain poorly constrained (see discussion in section 4.1.2). In section 4, we discuss a potential method for correcting shell $\delta^{13}\text{C}$ so shell profiles only reflect $\delta^{13}\text{C}_{\text{DIC}}$ variations, which contain the desired environmental information.

[10] Photosynthesis reactions preferentially make use of isotopically lighter $^{12}\text{CO}_2$. This has two implications: (1) at the ocean scale, as phytoplankton die this ^{12}C enriched organic matter sinks to the seafloor and is mineralized at depth. Deep waters upwelled along the Peruvian coast are therefore characterized by ^{13}C depleted DIC. (2) On a local scale, a phytoplankton bloom induces a ^{13}C enrichment of the surface water DIC during the growth

phase and a depletion of ^{13}C during the following organic matter degradation phase. Thus, if the isotopic carbon ratios in mollusk shells are representative of marine DIC, they may provide insights into the variability of upwelling activity and primary production at monthly to millennial timescales [Killingley and Berger, 1979; Jones and Allmon, 1995]. Furthermore, $\delta^{13}\text{C}_{\text{DIC}}$ of surface waters is also influenced by air-sea CO_2 exchange which depends on the difference of CO_2 partial pressure ($p\text{CO}_2$) between the atmosphere and the ocean [Lynch-Stieglitz *et al.*, 1995]. The relative contribution of these environmental controls over the $\delta^{13}\text{C}_{\text{DIC}}$ depends on local oceanographic features and will be discussed. The isotopic influence of one possible complicating factor, the influence of terrestrial freshwater runoff, is not significant in Peru because of the extreme aridity (Figure 2) and the weak discharge of coastal rivers (Worldclim 1.4 data set; available at <http://www.worldclim.org/current>), as confirmed in situ by monthly salinity measurements [Carré *et al.*, 2005a].

2. Material and Study Sites

[11] The bivalve *Mesodesma donacium* inhabits the subtidal to intertidal zone of sandy beaches along the

Table 1. Radiocarbon AMS Dates Measured on Charcoal Samples Associated to the Sampled *M. donacium* Shells^a

| Site | Sample Name | Number of Shells | ¹⁴ C Date (B.P.) | Laboratory Reference | Period |
|------|---------------------------------|------------------|-----------------------------|----------------------|-----------------|
| 15°S | Ica _{mod} | 15 | N/A | | Modern |
| | Ica _{inca} | 20 | 510 ± 40 | OS- 65628 | Inca |
| | Ica _{mH} | 20 | 5840 ± 35 | OS- 60543 | Middle Holocene |
| | | | 5900 ± 40 | OS- 60564 | |
| | | | 5940 ± 45 | OS- 60556 | |
| | | | 6070 ± 30 | OS- 60544 | |
| 18°S | QLB _{mod} ^b | 17 | N/A | | Modern |
| | QLB _{mH} | 13 | 6460 ± 60 | GifA-97287 | Middle Holocene |
| | | | 6510 ± 60 | GifA-97288 | |
| | | | 6630 ± 70 | GifA-97289 | |

^aThree time periods were represented by the shells collected; the modern day, Inca period and middle Holocene.

^bDates published by *Lavallée et al.* [1999].

Peruvian and Chilean coastline, and provides typical individual records of approximately one to two years [Carré *et al.*, 2005a]. Fossil mollusk shells were collected from two archeological sites along the Peruvian coastline: Rio Ica (14°52'S, 75°33'W) [Engel, 1957] and Quebrada de los Burros (QLB) (18°10'S, 70°38'W) [Lavallée *et al.*, 1999; Carré *et al.*, 2009] (Figure 2). Modern shell samples were collected from the respective nearby beaches in small mounds formed by fishermen activity during the second half of the 20th century. The sample size ranged from 13 to 20 shells (Table 1). Preservation of these historical shells was particularly high (as indicated by the remains of preserved organic matter) due to the extremely arid Peruvian coastline which receives precipitation of less than 20 mm yr⁻¹ (Worldclim 1.4 data set). Sample horizons of the archeological sites were dated by radiocarbon AMS measurements on charcoal fragments recovered among shell material (Table 1). A total of 85 shells were analyzed.

3. Methods

3.1. Shell Preparation and Microsampling

[12] Mollusk shells were embedded in polyester resin and radially sectioned using a diamond wire saw. Sections 1 mm thick were mounted onto glass slides and polished before sampling of the outer shell layer, along the direction of growth, with a MicromillTM automated micro-sampler. Each micro-sample constituted about 0.1 mg of powdered calcium carbonate, and represented about one month of shell growth based on shell inner growth lines (see Carré *et al.* [2005a, 2009] for details about sclero-chronology). With this technique, occasional areas of recrystallized carbonate located on the shell

surface can be identified by their color and avoided in the microsampling. Despite the high spatial control of the micro-sampler, an uncertainty remained over the identification of tidal growth lines and thus in the temporal resolution. The time span represented by a single micro-sample ranged between 0.5 to 2 months. Based on the $\delta^{18}\text{O}$ profiles and the number of micro-samples in a peak-to-peak 1 year cycle, the average time resolution of shell isotopic signals was re-estimated to be ~1.1 months.

3.2. Isotopic Analyses

[13] Approximately 0.05 mg of aragonite powder was sub-sampled from every micro-sample and analyzed for carbon ($\delta^{13}\text{C}$) and oxygen ($\delta^{18}\text{O}$) stable isotope composition with a Kiel III carbonate device coupled to a Finnigan Delta Plus isotope ratio mass spectrometer. The carbonate device drops excess 100% phosphoric acid onto calcium carbonate samples held at 70°C. Measurement reproducibility was 0.04‰ for $\delta^{13}\text{C}$ and 0.07‰ for $\delta^{18}\text{O}$ based on routine analyses quality control calcite standards. Isotopic values were placed on the VPDB scale by measurement against internal laboratory calcite standards that were measured against the international standards NBS19 and LSVEC [Verkouteren, 1999] for $\delta^{13}\text{C}$ and NBS19 and NBS18 for $\delta^{18}\text{O}$.

4. Results and Discussion

4.1. Influences on Shell $\delta^{13}\text{C}$

[14] Besides the seawater $\delta^{13}\text{C}_{\text{DIC}}$, mollusk shell aragonite $\delta^{13}\text{C}$ may also be influenced by kinetic fractionation, temperature, and the contribution of metabolic (also referred to as respired) carbon. We discuss below these influences in the conditions of our study.

4.1.1. Kinetic Effect

[15] A kinetic effect can be diagnosed by highly depleted values and a strong positive correlation between shell $\delta^{13}\text{C}$ and $\delta^{18}\text{O}$ [McConnaughey *et al.*, 1997]. Since this was not observed in *M. donacium* shells, we discounted the influence of a significant kinetic effect in our study.

4.1.2. Temperature Influence

[16] From the analysis of seawater $\delta^{13}\text{C}_{\text{DIC}}$ and aragonite $\delta^{13}\text{C}$ in several mollusk species, Grossman and Ku [1986] calculated empirical equations of the temperature dependent carbon fractionation in biogenic aragonite for *Hoeglundinae* and mollusks between 2.6 and 22°C:

$$\epsilon_{\text{Hoeg-DIC}}^{13}(\text{‰}) = 2.40 - 0.108 \cdot T(\text{°C}) \quad (R = 0.89, N = 52) \quad (1)$$

$$\epsilon_{\text{mollusk-DIC}}^{13}(\text{‰}) = 2.66 - 0.131 \cdot T(\text{°C}) \quad (R = 0.82, N = 26) \quad (2)$$

Later, Romanek *et al.* [1992] studied carbon fractionation of inorganic aragonite and calcite and found no temperature dependence for the aragonite- HCO_3^- fractionation, suggesting that “*aragonite-secreting taxa are influenced by temperature-dependent biological disequilibrium effects (“vital effects”).*” After this temperature dependence observed by Grossman and Ku [1986] was qualified “vital effect,” most researchers studying carbon stable isotopes in mollusk shells used the fractionation factor calculated by Romanek *et al.* [1992] and considered that carbon isotopes in biogenic aragonite were not influenced by temperature [McConnaughey *et al.*, 1997; Lorrain *et al.*, 2004; McConnaughey and Gillikin, 2008; Gillikin *et al.*, 2006a; Lartaud *et al.*, 2010].

[17] In contrast to these researchers, we have returned to the Grossman and Ku [1986] equation (2) for three reasons: (1) the empirical data set indicates a highly statistically significant, yet currently mechanically undefined relationship between temperature and $\epsilon_{\text{mollusk-DIC}}^{13}$; (2) as far as we know, no published data set using biogenic aragonite has invalidated this model, and (3) since we are studying biogenic aragonite, Grossman and Ku [1986] model is more appropriate than Romanek *et al.* [1992] model on inorganic aragonite. To support this latter reason, it seems important to remind that the mineralization processes for biogenic and inorganic aragonite are very different chemically and thermodynamically. First, aragonite does not spontane-

ously precipitate in the ocean and only exists because of shell organic matrix [Watabe and Wilbur, 1960; Suzuki *et al.*, 2009]. The crystal growth in shells is fully biologically controlled (timing, place, rate, and directions) through complex interactions with a large range of multifunctional proteins that constitute the shell organic matrix [Watabe and Wilbur, 1960; Wheeler *et al.*, 1981; Addadi and Weiner, 1992; Marin and Luquet, 2004; Marin *et al.*, 2007; Suzuki *et al.*, 2009]. The processes of organic aragonite precipitation involves the catalytic action of enzymes [Bevelander and Benzer, 1948; Freeman and Wilbur, 1948; Marxen *et al.*, 2003; Marin and Luquet, 2004] which have a temperature dependent efficiency [Somero, 1969; Ikemoto, 1975; Hall, 1985; Pick and Karlsh, 1982; Wolfenden *et al.*, 1999]. Enzymatic reactions also induce a temperature dependent isotopic fractionation [Northrop, 1981; Schowen and Schowen, 1981; Liu and Warshel, 2007]. A temperature-dependent ^{13}C fractionation between HCO_3^- and the other inorganic carbon species may also be involved. Studying the mechanisms behind a $\delta^{13}\text{C}$ temperature effect in biogenic aragonite is beyond the scope of this paper, but it is clear that the question requires further research. The correlation between temperature and $\epsilon_{\text{mollusk-DIC}}^{13}$ may only be indirect and not causal but it still reveals the existence of a chemical and/or biological effect that can be estimated through temperature. The fact that Grossman and Ku [1986] calculated a similar equation for the foraminifera *Hoeglunidae* and twelve species of mollusks suggests that this effect may indeed be characteristic of a large range of aragonite-secreting organisms.

[18] In light of these observations and until further results suggest otherwise, correcting our mollusk shell $\delta^{13}\text{C}$ data for an expected and quantified temperature effect using $\delta^{18}\text{O}$ based temperature reconstructions [Carré *et al.*, 2005a] was selected as the most suitable course of action.

4.1.3. Correcting Shell $\delta^{13}\text{C}$ for the Temperature Effect

[19] We analyzed the oxygen isotopic composition of seawater samples from the southern coast of Peru collected between 2002 and 2007 (Table 2). In the Rio Ica area, average isotopic values were $\delta^{18}\text{O}_{\text{seawater}} = 0.26\text{‰}_{\text{V-SMOW}}$ ($\sigma = 0.11$, $N = 8$), whereas in the QLB area it was estimated at $\delta^{18}\text{O}_{\text{seawater}} = 0.21\text{‰}_{\text{V-SMOW}}$ ($\sigma = 0.15$, $N = 20$). The water $\delta^{18}\text{O}$ on this coast displays little variation and no seasonality because it is not significantly affected by freshwater input. This was confirmed in modern

Table 2. Seawater $\delta^{18}\text{O}$ Data

| Coastal Site | Lat. | Long. | Date (dd-mm-yy) | $\delta^{18}\text{O}$ (% V-SMOW) |
|-----------------|---------|---------|-----------------|----------------------------------|
| Lagunillas | 13°55'S | 76°19'W | 09-08-03 | 0.28 |
| Rio Ica beach | 14°52'S | 75°34'W | 11-02-07 | 0.39 |
| | | | 07-12-07 | 0.26 |
| Puerto Caballas | 14°56'S | 75°29'W | 15-12-07 | 0.32 |
| Puerto Lomas | 15°33'S | 75°50'W | 13-08-02 | 0.03 |
| | | | 19-12-07 | 0.38 |
| Tanaka | 15°43'S | 74°28'W | 25-01-03 | 0.19 |
| | | | 16-12-07 | 0.25 |
| Ilo | 17°38'S | 71°21'W | 22-08-02 | 0.34 |
| | | | 06-11-02 | -0.07 |
| | | | 04-12-02 | 0.10 |
| | | | 08-01-03 | 0.18 |
| | | | 07-02-03 | 0.04 |
| | | | 16-06-03 | 0.14 |
| | | | 16-07-03 | 0.26 |
| | | | 04-08-03 | 0.33 |
| | | | 03-09-03 | 0.35 |
| | | | 10-10-03 | 0.32 |
| | | | 14-11-03 | 0.08 |
| | | | 12-12-03 | 0.03 |
| | | | 12-01-04 | 0.47 |
| | | | 11-02-04 | 0.16 |
| | | | 17-03-04 | 0.3 |
| | | | 12-04-04 | 0.11 |
| QLB | 18°01'S | 70°50'W | 19-11-07 | 0.32 |
| Llostay | 18°10'S | 70°39'W | 27-01-03 | -0.03 |
| | | | 08-11-07 | 0.33 |
| | | | 13-11-07 | 0.37 |

conditions by seawater $\delta^{18}\text{O}$ measurements (Table 2) and monthly salinity time series [Carré et al., 2005a]. Despite some variations of humidity, the coastal climate remained arid or semi-arid in southern Peru [Eitel et al., 2005; Kuentz et al., 2012] and precipitation was reduced in the Andes during the middle Holocene [Baker et al., 2001; Rein et al., 2005]. It can thus be considered constant in average throughout the year, and shell $\delta^{18}\text{O}$ variations can be interpreted as reflecting changes in SST. The middle Holocene shell $\delta^{18}\text{O}$ values were also corrected for changes in the mean ocean water $\delta^{18}\text{O}$ caused by variations in ice volume. This was conducted using the sea level curve of Lambeck and Chappell [2001] with an estimate of a 1.05‰ decrease in oceanic $\delta^{18}\text{O}$ between the Last Glacial Maximum and the present-day [Duplessy et al., 2002]. A correction of 0.049‰ and 0.079‰ was applied to mid-Holocene shells of Rio Ica and QLB respectively. Paleotemperature values were calculated using the Carré et al. [2005a] transfer equation. Temperature-related carbon fractionation was calculated using equation (2) and isotopic temperature estimates, and then subtracted from shell $\delta^{13}\text{C}$ values (Figure 3). We therefore generated signal of

corrected $\delta^{13}\text{C}$ values ($\delta^{13}\text{C}_{\text{corr}}$) which are primarily influenced by the variations of $\delta^{13}\text{C}_{\text{DIC}}$ and the contribution of metabolic carbon. The standard error of $\delta^{13}\text{C}_{\text{corr}}$ was estimated at 0.17‰ (1σ) and combines analytical errors on both shell $\delta^{13}\text{C}$ and $\delta^{18}\text{O}$ and the monthly variability of water $\delta^{18}\text{O}$. The 85 individual corrected $\delta^{13}\text{C}$ profiles are represented in Figure 4 and span from ~10 months to ~24 months for the larger shells.

4.2. The Influence of Metabolic Carbon

[20] The relative proportion of carbon of metabolic versus environmental origin is an uncertain parameter that may strongly vary with species and environment [Tanaka et al., 1986; Klein et al., 1996; McConnaughey et al., 1997; Gillikin et al., 2006a, 2007; McConnaughey and Gillikin, 2008]. In early studies, authors proposed that shell $\delta^{13}\text{C}$ variations mainly reflected $\delta^{13}\text{C}_{\text{DIC}}$ and could therefore be used as paleoenvironmental tracers [Mook and Vogel, 1968; Mook, 1971; Killingley and Berger, 1979; Arthur et al., 1983; Krantz et al., 1987, 1988;

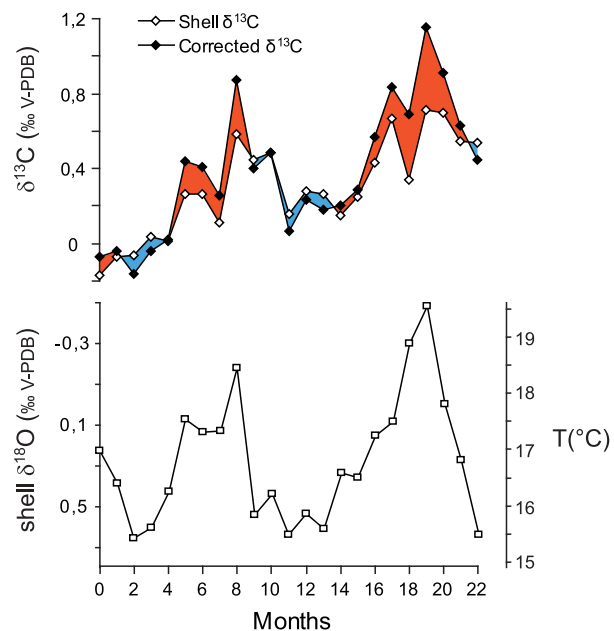


Figure 3. $\delta^{13}\text{C}$ (open diamonds) and $\delta^{18}\text{O}$ (open squares) measured with a monthly resolution along the growth axis of a modern shell (brmd24) collected live in June 2003 on the Llostay beach (close to the QLB site). $\delta^{18}\text{O}$ values were converted to temperature using Carré et al.'s [2005a] equation and a water $\delta^{18}\text{O}$ value of 0.18‰(V-SMOW). $\delta^{13}\text{C}_{\text{corr}}$ values (closed diamonds) were calculated from shell $\delta^{13}\text{C}$ corrected from the temperature fractionation effect and the Suess effect. Positive corrections appear in red and negative corrections in blue.

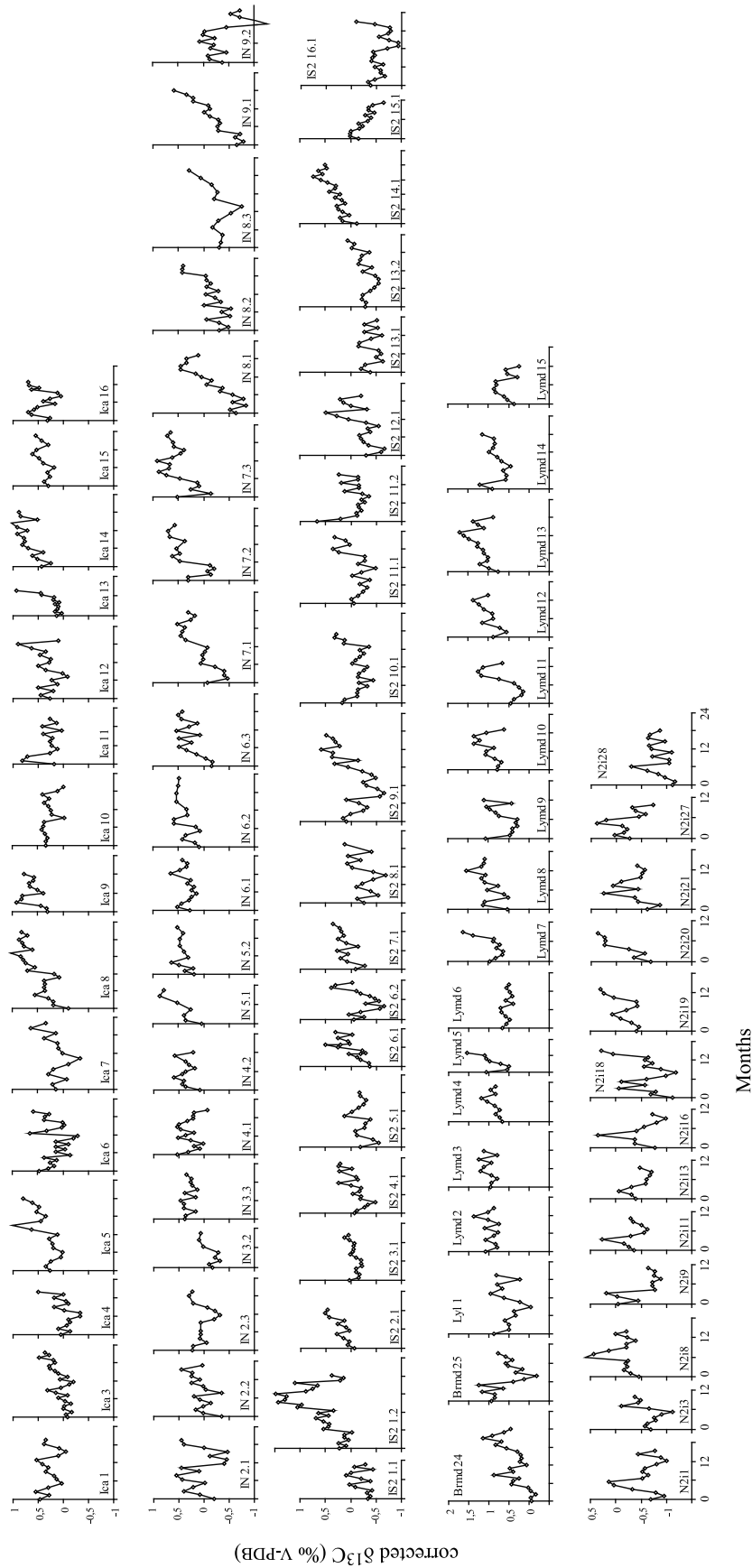


Figure 4. $\delta^{13}\text{C}$ profiles for all shells corrected for the temperature effect and for the Suess effect (modern shells only). Isotopic values were positioned on a monthly time axis after re-evaluating the mean microsampling resolution for every shell.

Table 3. Seawater $\delta^{13}\text{C}_{\text{DIC}}$ Data

| Coastal Site | Lat. | Long. | Date (dd-mm-yy) | $\delta^{13}\text{C}_{\text{DIC}}$ (‰ V-PDB) |
|--------------|---------|---------|--------------------|---|
| Lagunillas | 13°55'S | 76°19'W | 23-11-01 | -0.15 |
| | | | 23-11-01 | -0.46 |
| | | | 20-06-03 | -0.46 |
| | | | 21-06-03 | -0.25 |
| San Juan | 15°21'S | 75°10'W | 28-11-01 | -1.39 |
| | | | 28-11-01 | 0.17 |
| Pocoma | 17°25'S | 71°23'W | 25-11-01 | -0.36 |
| | | | 25-11-01 | 0.07 |
| | | | 16-06-03 | 0.21 |
| | | | 16-06-03 | 0.21 |
| | | | 16-12-03 | 0.04 |
| | | | 17-01-04 | 0.22 |
| | | | 15-02-04 | 0.13 |
| | | | 28-03-04 | 0.21 |
| Ilo | 17°38'S | 71°21'W | 16-09-04 | 0.23 |
| | | | 27-11-01 | -1.04 |
| | | | 27-11-01 | -0.37 |

Bemis and Geary, 1996]. The contribution of metabolic carbon was estimated to be <10% in most marine calcified skeletons [*McConnaughey et al.*, 1997; *McConnaughey and Gillikin*, 2008]. Because the $\delta^{13}\text{C}$ of respired carbon is highly depleted ($\sim -20\%$) compared to DIC ($\sim 1\%$), 10% variations of metabolic carbon contribution could have significant effects of $\sim 2\%$ on shell isotopic signature [*Gillikin et al.*, 2006a]. Besides an average contribution of metabolic carbon, $\delta^{13}\text{C}$ variations within shells have also been attributed to variations in this metabolic component. Systematic decreasing trends in shell $\delta^{13}\text{C}$ through ontogeny have been reported in mollusk shells [*Romanek and Grossman*, 1989; *Keller et al.*, 2002; *Elliot et al.*, 2003]. *Lorrain et al.* [2004] showed that in scallop shells, these ontogenetic $\delta^{13}\text{C}$ trends were due to increasing contribution of respired carbon with the body size. An influence of food availability was also suggested by *Van der Putten et al.* [2000] because of decreasing $\delta^{13}\text{C}$ values associated with Mn and Ba peaks which are believed to be related to phytoplankton blooms [*Stecher et al.* 1996; *Gillikin et al.*, 2006b; *Thébault et al.*, 2009]. However, the majority of the shell $\delta^{13}\text{C}$ signal was associated with shell transplantation to a locality under larger influence of freshwater and thus with lower $\delta^{13}\text{C}_{\text{DIC}}$ values. Recently, *Lartaud et al.* [2010] observed decreased shell $\delta^{13}\text{C}$ associated with food availability in cultured *Crassostrea gigas*, but a strong positive correlation with shell $\delta^{18}\text{O}$ suggested the possible presence of kinetic effect, and these isotopic depletions were not observed in natural conditions. Based on the *Pecten maximus* isotopic records published by *Lorrain et al.* [2004], *Chauvaud et al.* [2011] proposed a model where

intraseasonal shell $\delta^{13}\text{C}$ variations were mainly due to metabolic effect modulated by food availability. This model, however, cannot be generalized since it did not fit the other *P. maximus* records published in the same article, where shell $\delta^{13}\text{C}$ variations followed a classic $\delta^{13}\text{C}_{\text{DIC}}$ seasonal cycle, with low values during winter for the freshwater input and high values in spring during the peak of phytoplankton productivity. In summary, there remains little evidence for significant seasonal variations of metabolic carbon contribution in mollusk shells. The contribution of metabolic carbon in mollusk shells can be estimated using the following equation from *McConnaughey et al.* [1997]:

$$M \cdot \delta^{13}\text{C}_{\text{meta}} + (1 - M) \cdot \delta^{13}\text{C}_{\text{Env}} = \delta^{13}\text{C}_{\text{shell}} - \epsilon_{\text{arag-HCO}_3^-} \quad (3)$$

Where M is the fraction of metabolic carbon, $\delta^{13}\text{C}_{\text{meta}}$, $\delta^{13}\text{C}_{\text{Env}}$, and $\delta^{13}\text{C}_{\text{shell}}$ the isotopic value of the metabolic HCO_3^- , environmental HCO_3^- and shell aragonite respectively. $\epsilon_{\text{arag-HCO}_3^-}$ is the enrichment factor between shell aragonite and HCO_3^- in the extrapalleal fluid. When using this equation, most authors assume that $\epsilon_{\text{arag-HCO}_3^-}$ is constant and equal to the enrichment factor calculated for inorganic aragonite ($2.7 \pm 0.6\%$). Further research is needed to demonstrate the validity of this assumption. Because of the biological influence in the mineralization process, the average enrichment factor may be different for shell aragonite, and may also vary during the mollusk life with environmental or biological factors. Following the discussion of section 4.1.2, considering a temperature dependence of the enrichment factor may be a first improvement in the estimation of M.

[21] We used an approximate value of -20% for the metabolic carbon. The $\delta^{13}\text{C}_{\text{DIC}}$ value of sea surface water on the southern Peruvian coast was estimated at -0.18% ($\sigma = 0.47\%$) based on 17 measurements between 14°S and 18°S in the 2001–2004 period (Table 3). The average $\delta^{13}\text{C}_{\text{shell}}$ value was 0.17% for the Ica modern shells and 0.58% for the Llostay modern shells. Using an enrichment factor calculated from the *Grossman and Ku* [1986] relationship for biogenic aragonite and an average temperature value of 17°C , the estimates of the metabolic contribution were 2% for Ica and 0.2% for Llostay.

[22] We concluded that $\delta^{13}\text{C}$ variations in *M. donacium* shells are not significantly affected by inner variations of the metabolic effect because of three observations: (1) the estimates of the metabolic carbon percentages in *M. donacium* were low, (2) no systematic ontogenetic decreasing trend was observed

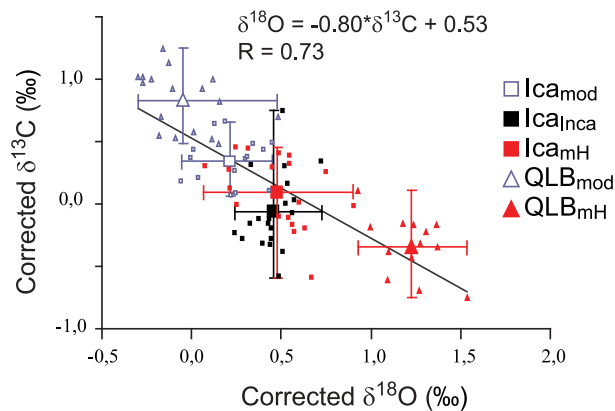


Figure 5. Mean value of corrected $\delta^{13}\text{C}$ versus mean value of $\delta^{18}\text{O}$ (corrected for ice volume effect in mid Holocene samples) for individual shells (small symbols) and for the five whole samples (large symbols). Bars indicate the range of mean values of individual shells within a sample. The least square linear regression was calculated from the individual shells mean values ($N = 85$).

in the individual carbon isotopic signals, (3) no $\delta^{13}\text{C}$ depleted values were associated to Mn and Ba peaks in *M. donacium* modern shells (shells brmd21 and brmd24 in the work of Carré *et al.* [2005a, 2006]). As a result we suggest that $\delta^{13}\text{C}_{\text{corr}}$ profiles in Figure 3 mainly reflect variations of seawater $\delta^{13}\text{C}_{\text{DIC}}$.

4.3. Correcting for the Suess Effect

[23] Since the industrial revolution, the combustion of fossil fuels has provided an additional source of ^{12}C enriched carbon into the atmosphere, decreasing the $\delta^{13}\text{C}$ global value of the atmospheric CO_2 . This anthropogenic influence is referred to as the Suess effect. This additional ^{12}C diffuses into the ocean and has reduced the surface ocean $\delta^{13}\text{C}$ since the industrial revolution [Keeling, 1979; Quay *et al.*, 1992; Bacastow *et al.*, 1996]. To allow comparisons between the modern day and preindustrial periods, this anthropogenic effect should be removed from modern shell $\delta^{13}\text{C}$ values. The amplitude of the Suess effect varies with local oceanographic characteristics. Based on estimations of anthropogenic carbon concentration in the South East Pacific [Goyet *et al.*, 2009], we calculated a Suess effect correction of 0.5‰ for the Peruvian coast. This value is lower than the Suess effect measured in the Caribbean (0.9‰) and in New Caledonia (0.7‰) by Böhm *et al.* [1996], which is consistent with a larger contribution of deep water in Peru. We tested whether the seasonal variation of the coastal upwelling strength could induce seasonal variations of the Suess effect that would dampen the shell $\delta^{13}\text{C}$

amplitude. Since no significant difference was found between $\delta^{13}\text{C}$ annual amplitude of modern and fossil shells, we assumed this potential effect was not significant. An example of a modern shell $\delta^{13}\text{C}$ signal corrected for the Suess effect and the temperature effect is shown in Figure 3.

4.4. Stable Isotopes and the Intensity of Coastal Upwelling

[24] Considering the assumptions discussed in sections 4.1 and 4.2, shell $\delta^{13}\text{C}_{\text{corr}}$ reflect $\delta^{13}\text{C}_{\text{DIC}}$. The full data set plotted together (Figure 5) shows a strong linear correlation between mean $\delta^{13}\text{C}_{\text{corr}}$ and mean $\delta^{18}\text{O}$ values, with a slope value of -0.80 . Mean values of both $\delta^{13}\text{C}_{\text{DIC}}$ and $\delta^{18}\text{O}_{\text{carbonates}}$ are expected to provide an indication of the background signal generated by the presence of deep water. Deep water brought to the surface by coastal upwelling is characterized by lower temperatures (corresponding to higher $\delta^{18}\text{O}_{\text{carbonates}}$ values) associated with lower $\delta^{13}\text{C}_{\text{DIC}}$ readings.

[25] To test the hypothesis that the linear relationship between mean $\delta^{13}\text{C}_{\text{corr}}$ and $\delta^{18}\text{O}_{\text{carbonates}}$ which appears in our data set is related to the upwelling mean intensity, we compared it to the relationship between $\delta^{13}\text{C}_{\text{DIC}}$ and $\delta^{18}\text{O}_{\text{carbonates}}$ expected along a depth profile within the 100m surface layer using the following equation:

$$\frac{\partial(\delta^{13}\text{C}_{\text{DIC}})}{\partial(\delta^{18}\text{O}_{\text{carb.}})} = \left[\frac{\partial(\delta^{13}\text{C}_{\text{DIC}})}{\partial(D)} \right] \cdot \left[\frac{\partial(D)}{\partial(T)} \right] \cdot \left[\frac{\partial(T)}{\partial(\delta^{18}\text{O}_{\text{carb.}})} \right]_{M. donacium} \quad (4)$$

where D is the water depth (m), and T is the water temperature ($^{\circ}\text{C}$). $\delta^{13}\text{C}_{\text{DIC}}$ depth profiles measured by Quay *et al.* [2003] provide an average estimate of $6 \cdot 10^{-3} \text{‰m}^{-1}$ for $\partial(\delta^{13}\text{C}_{\text{DIC}})/\partial(D)$ in the 100m surface layer. The temperature-depth dependence $\partial(T)/\partial(D)$ is $\sim 0.03^{\circ}\text{Cm}^{-1}$ in the surface layer of the coastal Peru based on in situ measurements of IMARPE. $\partial(T)/\partial(\delta^{18}\text{O}_{\text{carb.}})$ in aragonite was estimated at $-3.66^{\circ}\text{C}/\text{‰}$ for *M. donacium* by Carré *et al.* [2005a]. A value of -0.73 is obtained from equation (4), very close to the slope value of -0.80 obtained from our data set (Figure 5). This result supports our hypothesis that the linear relationship between $\delta^{13}\text{C}_{\text{corr}}$ and $\delta^{18}\text{O}_{\text{carb}}$ mean values obtained from mollusk shells defines a gradient of influence of deep water, equivalent to a gradient of upwelling intensity. Our interpretation is also supported by temperature instrumental data indicating a stronger upwelling today at 15°S (sample ICA_{mod}) than at 18°S (sample QLB_{mod}) (Figures 1 and 5).

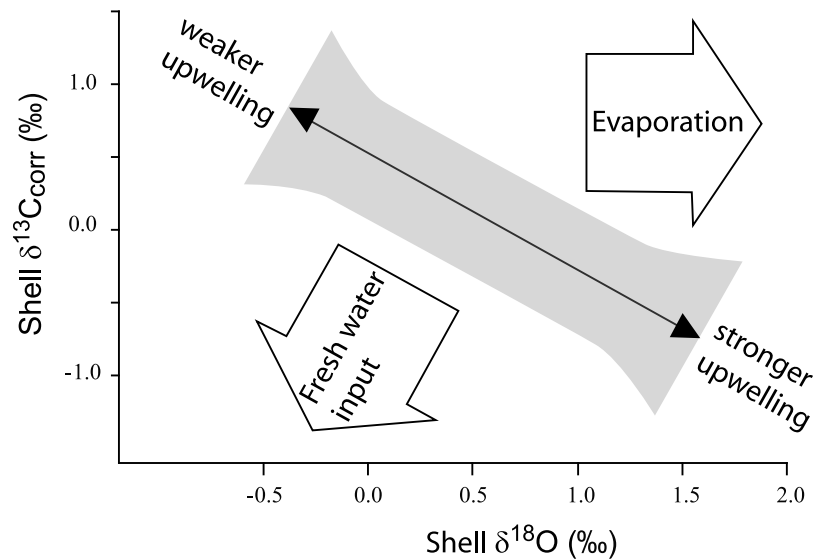


Figure 6. Schematic model of the upwelling-related relationship between mean shell $\delta^{18}\text{O}$ values and mean shell $\delta^{13}\text{C}_{\text{corr}}$ values. Deviations from this relationship may be due to evaporation effect or to continental fresh water influence.

[26] The linear relationship between average values of shell $\delta^{18}\text{O}$ and $\delta^{13}\text{C}_{\text{corr}}$ defines a coastal upwelling intensity axis (Figure 6). So far, and because of the complex influences of mollusk $\delta^{13}\text{C}$ signal, the local variations of paleoupwelling intensity were inferred from shell $\delta^{18}\text{O}$ [Carré et al., 2005b, 2012] based on the negative relationship between sea surface temperature and upwelling rate. Although this approach is generally accurate, additional influences on shell $\delta^{18}\text{O}$, such as evaporation or fresh water input, may lead to incorrect interpretations. The combination of shell $\delta^{18}\text{O}$ and $\delta^{13}\text{C}_{\text{corr}}$ and the position of average values relatively to the upwelling axis allow us to detect environmental influences. A position close to the upwelling $\delta^{18}\text{O} - \delta^{13}\text{C}_{\text{corr}}$ relationship suggest that upwelling rate is the major control of the average water geochemistry, whereas evaporative conditions (for instance in a close embayment) are indicated by a deviation toward $\delta^{18}\text{O}$ enrichment, and fresh water influence is indicated by a combined depletion of $\delta^{18}\text{O}$ and $\delta^{13}\text{C}_{\text{corr}}$ (Figure 6). The upwelling $\delta^{18}\text{O} - \delta^{13}\text{C}_{\text{corr}}$ relationship proposed here relies on a $\delta^{13}\text{C}_{\text{DIC}}$ -depth relationship, a temperature-depth relationship and a specific paleotemperature relationship (equation (3)); it is thus only valid for southern Peru and *M. donacium* shells although the method could be similarly applied with other species in other regions.

[27] The $\delta^{13}\text{C}$ and $\delta^{18}\text{O}$ signals confirm that coastal upwelling conditions were significantly stronger during the middle Holocene (Figure 5), which had been already suggested by independent paleoenvironmental results [Bétancourt et al., 2000; Holmgren

et al., 2001; Placzek et al., 2001; Rech et al., 2003; Fontugne et al., 2004; Koutavas and Sachs, 2008; Ortlieb et al., 2011]. Furthermore, during the middle Holocene, the strongest coastal upwelling was experienced at 18°S (Figure 5), whereas under modern conditions, upwelling intensity at 18°S is currently weaker than at 15°S. This result suggests a spatial reorganization of the intensity of coastal upwelling centers, possibly as a response to a different wind field.

4.5. Seasonal Signals of Stable Isotopes

[28] For modern samples, the average annual amplitudes of shell $\delta^{13}\text{C}_{\text{corr}}$ range from 0.72‰ (ICA_{mod}) to 0.85‰ (QLB_{mod}). In fossil samples, average annual $\delta^{13}\text{C}_{\text{corr}}$ amplitude is 0.80‰ for Ica_{Inca}, 0.83‰ for Ica_{mH}, and 0.99‰ for QLB_{mH}. The difference between these values is not statistically significant. For the whole Peruvian South coast, we obtain an average annual $\delta^{13}\text{C}_{\text{corr}}$ amplitude of 0.83‰. Trends in $\delta^{18}\text{O}$ follow the seasonal patterns of temperature, with low $\delta^{18}\text{O}$ values representing the warmer temperatures of austral summer (Figures 3 and 8). Although $\delta^{13}\text{C}_{\text{corr}}$ monthly signals exhibit a less pronounced seasonal pattern than $\delta^{18}\text{O}$, seasonal $\delta^{13}\text{C}_{\text{corr}}$ variations are generally in phase with, or lag slightly behind, temperature. Enriched $\delta^{13}\text{C}_{\text{corr}}$ values are generally recorded in summer and depleted values are recorded during winter. If trends in shell $\delta^{13}\text{C}_{\text{corr}}$ represent $\delta^{13}\text{C}_{\text{DIC}}$ variations (section 4.3), then mollusk shells are recording seasonal fluctuations of $\delta^{13}\text{C}_{\text{DIC}}$ in coastal waters. At the seasonal scale, $\delta^{13}\text{C}_{\text{DIC}}$ is controlled by a combination of

(1) primary productivity, (2) upwelling seasonality, and (3) sea-atmosphere CO₂ exchange.

[29] Carbon isotope fractionation occurs during sea-atmosphere CO₂ exchange. ¹²CO₂ is favored in the outgassing reaction that induces an enrichment of ^{δ¹³C_{DIC}} within surface waters. This effect increases with the CO₂ flux, which depends on the pCO₂ difference between the atmosphere and the surface water. Carbon isotopic equilibration takes approximately 10 years therefore ^{δ¹³C_{DIC}} is never in isotopic equilibrium with the atmosphere along the Peruvian coast where the surface water is constantly replaced by deep water through upwelling. At the seasonal scale, carbon fractionation in sea-atmosphere exchange is mainly due to kinetic effects [Lynch-Stieglitz *et al.*, 1995]. The net CO₂ flux of the Peruvian coast is toward the atmosphere due to the very high pCO₂ values that characterize upwelled waters. The CO₂ flux, and therefore the fractionation effect, is strongest during the winter when ΔpCO₂ may reach 1000 ppm and weakest during the summer when ΔpCO₂ is closer to 0 ppm. Therefore, the effect of air-sea CO₂ exchange on the ^{δ¹³C_{DIC}} is enrichment during the winter and depletion during the summer. Since this is opposite to most trends recorded in mollusk shells, we conclude that air-sea CO₂ exchange have a minor control on seasonal ^{δ¹³C_{DIC}} variations.

[30] In contrast to air-sea exchange, seasonal variability in the intensity of coastal upwelling would produce ^{δ¹³C_{DIC}} in phase with the temperature annual cycle. This effect can be estimated from the seasonal variations of the thermocline depth and the trend in ^{δ¹³C_{DIC}}-depth relationship. In situ measurements reveal that the amplitude of the thermocline seasonal vertical movement in non-El Niño years is ~30m. Considering a 6.10⁻³ ‰ m⁻¹ depletion for ^{δ¹³C_{DIC}} with depth [Quay *et al.*, 2003], the effect of upwelling seasonality is estimated to be about 0.2‰, which cannot explain the 0.83‰ of variations observed in shell samples.

[31] The primary control for ^{δ¹³C_{DIC}} seasonal variations would therefore be the remaining variable: primary productivity. Productivity peaks induce ^{δ¹³C} enrichment of the DIC in the surface layer, which would generally occur during summer as indicated by in situ and satellite chlorophyll *a* measurements [Echevin *et al.*, 2008]. The phasing of the productivity effect is thus in agreement with ^{δ¹³C_{DIC}} variations measured in mollusk shells. To further test this hypothesis, we used the relationship between ^{δ¹³C_{DIC}} and PO₄ in the ocean published by Broecker and Maier-Reimer [1992], which allows

for an estimate on the productivity effect on ^{δ¹³C_{DIC}} without air-sea exchange:

$$\delta^{13}\text{C}_{\text{DIC}} = 2.7 - 1.1 \times \text{PO}_4 \quad (5)$$

The seasonal variation in PO₄ at 15°S on the Peruvian coast is ~0.8 μg.L⁻¹ (measured by IMARPE in oceanographic cruises between 1964 and 2008, excluding El Niño years), which corresponds to a ^{δ¹³C_{DIC}} seasonal variation of ~0.9‰ based on equation (5). This value is very close to the amplitude of ^{δ¹³C_{DIC}} recorded in mollusk shells, which supports our hypothesis that the dominant control on seasonal variations of ^{δ¹³C_{DIC}} recorded by shell ^{δ¹³C_{corr}} is primary productivity.

[32] In order to quantitatively estimate the seasonal timing of phytoplankton blooms and its variability with sites and periods, lag periods between ^{δ¹³C_{corr}} and ^{δ¹⁸O} were evaluated using cross-correlation. Correlations between ^{δ¹³C_{corr}} and ^{δ¹⁸O} trends of individual shells were evaluated between lag periods of ±6 data points. The lag corresponding to the highest positive correlation between isotopic signals, multiplied by the microsampling resolution, was interpreted as the monthly time difference between the productivity bloom (^{δ¹³C_{corr}} maximum) and the February temperature maximum/August temperature minimum for positive and negative correlations respectively (Figure 7). Compared to a simple peak-to-peak distance between ^{δ¹³C_{corr}} and ^{δ¹⁸O}, this technique takes into account the full shape of the signal and is thus more reliable for estimating a time lag. The seasonal timing of blooms determined from each shell were then classified into austral spring (October–December), summer (January–March), autumn (April–June) or winter (July–September).

[33] The seasonal timings of phytoplankton blooms evaluated by this new technique were plotted as frequency distributions for the middle Holocene, the Inca period and modern day (Figure 8). Modern shell samples from both locations reveal that phytoplankton blooms were most common during austral summer, in agreement with chlorophyll *a* data (Figure 1) [Thomas *et al.*, 1994; Echevin *et al.*, 2008], which supports the reliability of the technique for paleoenvironmental analysis.

4.6. Past Seasonal Dynamics of Phytoplankton Bloom

[34] Based on our assumptions and method, the lag between ^{δ¹³C_{corr}} and ^{δ¹⁸O} seasonal signals in individual shells provides an indication of the season of the main phytoplankton bloom (Figure 7). In our

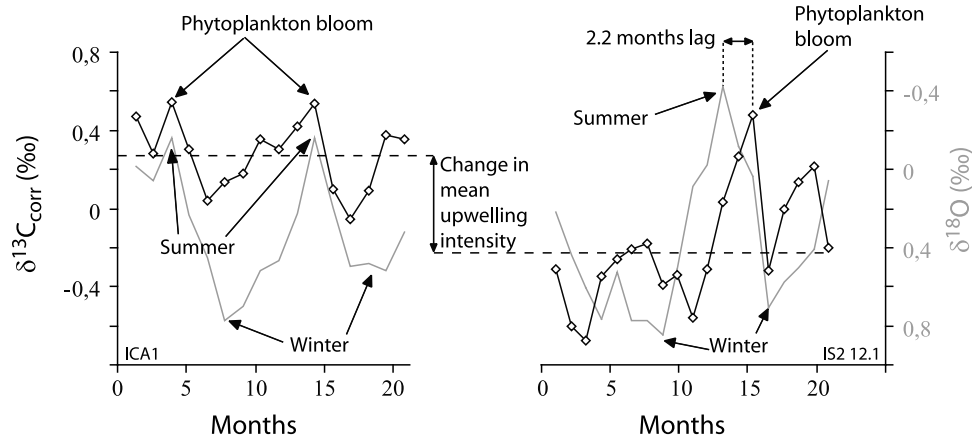


Figure 7. The $\delta^{13}\text{C}_{\text{corr}}$ (diamonds) and $\delta^{18}\text{O}$ (gray line) profiles of two shells of the same area: a modern shell from ICA_{mod} (ICA1) and a fossil shell from ICA_{Inca} (IS2 12.1). Mean $\delta^{13}\text{C}_{\text{corr}}$ values are indicated by dashed lines. The difference between mean values is due to the mean intensity of the coastal upwelling. Summers (February) and winters (August) were identified from the $\delta^{18}\text{O}$ curves. At the seasonal scale, $\delta^{13}\text{C}_{\text{corr}}$ maxima correspond to ^{13}C enrichment phases of the DIC due to phytoplankton blooms. Lags between $\delta^{13}\text{C}_{\text{corr}}$ and $\delta^{18}\text{O}$ are estimated by cross-correlation. A 2.2 month lag was estimated for the fossil shell, indicating a phytoplankton bloom in fall, while no lag was found in the modern shell, indicating a phytoplankton bloom in summer.

case study, we show that modern and fossil samples show similar coastal phytoplankton dynamics at 15°S: bloom development appears to coincide mainly with summer, which corresponds to the warmer SSTs and autumn, which correspond to the onset of upwelling strengthening (Figure 8). This would imply that light is the first limiting factor for phytoplankton growth and upwelled nutrients are a second limiting factor. At 18°S (QLB site), the modern and middle Holocene samples also show a predominance of summer blooms. However, an increase in spring blooms and an absence of fall blooms are also observed. This result suggests that light was the only limiting factor at that time and that upwelled nutrients were not at all limiting, which is consistent with stronger upwelling mean conditions.

[35] The influences of gas air-sea exchanges, upwelling seasonality, and biological effects, were likely secondary in our case study, but they still exist and might in some circumstances be predominant in the $\delta^{13}\text{C}_{\text{corr}}$ signal, inducing thus some noise in the final result. The precision of this technique for evaluating the seasonal timing of phytoplankton blooms is also limited by the variability of the temperature profile and the uncertainties in the $\delta^{18}\text{O}$ signal. Finally, the method is based on an isotopic model that could be improved by comparing mollusk shell profiles with in situ weekly measurements of marine $\delta^{13}\text{C}_{\text{DIC}}$, productivity, and wind stress over an annual cycle. Such calibration work may allow for more detailed reconstructions. Nevertheless, mollusk stable isotopes could potentially pro-

vide new valuable insights into long-term variability of coastal seasonal biogeochemical processes.

5. Conclusions

[36] In this study we proposed a new method to evaluate past variations (1) of the mean intensity of

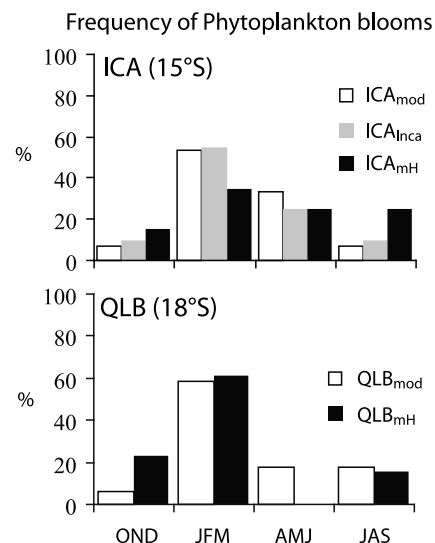


Figure 8. Frequency distributions of the season of occurrence of the main phytoplankton bloom. The bloom dates were determined by the lag between shell $\delta^{13}\text{C}_{\text{corr}}$ and $\delta^{18}\text{O}$, assuming $\delta^{18}\text{O}$ seasonal minima correspond to February (see Figure 7). Frequencies were defined as the percentage of shells in a sample. A comparison was made between modern (mod) and fossil (Inca and mH) samples for both study sites.

the Peruvian coastal upwelling and (2) of the seasonal timing of phytoplankton blooms. This method uses a combination of the monthly carbon and oxygen isotopic signal preserved in fossil shells of *M. donacium*. Our method involves a re-evaluation of the paradigm that considers that the ^{13}C enrichment factor between shell aragonite and HCO_3^- is constant and equal to the enrichment factor of inorganic aragonite. We considered that it is more likely to vary with temperature following *Grossman and Ku's* [1986] empirical model, although the mechanism remains unknown. After being corrected for temperature and Suess effects, shell $\delta^{13}\text{C}_{\text{corr}}$ variations are believed to primarily reflect $\delta^{13}\text{C}_{\text{DIC}}$ variations. At the centennial to millennial scale, $\delta^{13}\text{C}_{\text{DIC}}$ mean values are primarily affected by the mean intensity of the upwelling, while primary productivity is the main factor controlling seasonal $\delta^{13}\text{C}_{\text{DIC}}$ variations.

[37] Five shell samples from the southern Peruvian coast were analyzed and show a strong linear correlation between average values of shell $\delta^{13}\text{C}_{\text{corr}}$ and $\delta^{18}\text{O}$, similar to the expected relationship along a gradient of influence of deep water, which represents a gradient of upwelling intensity. We then proposed a proxy model to estimate the past intensity of the coastal upwelling in Peru. This method could bring additional independent information valuable to interpret paleoproductivity changes reconstructed from marine sediment of the nearby continental shelf. Results obtained on fossil samples from the middle Holocene suggest an increase of the upwelling during this period, consistent with existing independent paleoenvironmental reconstructions. Additionally, fossil shells show a spatial reorganization of upwelling centers along the South Peruvian coast. At the seasonal scale, shell $\delta^{13}\text{C}_{\text{corr}}$ enrichment was interpreted as the indication of a phytoplankton bloom. Bloom seasonal timings may thus be estimated by the lag between shell $\delta^{13}\text{C}_{\text{corr}}$ and the annual temperature cycle reproduced by shell $\delta^{18}\text{O}$ monthly variations. The results obtained with two modern shell samples indicate phytoplankton blooms occurring during summer and fall, consistently with in situ productivity observations. The timing of productivity blooms was similar in fossil samples suggesting little change in limiting factors of phytoplankton growth. One strength of this study lies in the large amount of data which averages out a significant part of random uncertainty and provides statistical robustness to the results. Although this work is only valid for southern Peru and the mollusk species *M. donacium*, this approach could be developed in other similar areas like

the Benguela current system where the upwelling maintains arid conditions on the coast, and where numerous fossil shell middens are preserved.

[38] However, while our interpretation in this case study is arguably the most parsimonious hypothesis with regards to actual knowledge of carbon isotopes in mollusk shells, it is clear that further investigation is needed to understand the factors that influence the carbon isotopic fractionation in biogenic aragonite. We estimated here that the enrichment factor $\epsilon_{\text{arag-HCO}_3^-}$ is more likely to be not constant in biogenic aragonite, which should lead to a re-evaluation of the contribution of the metabolic carbon in the shell formation.

Acknowledgments

[39] We are grateful to D. Lavallée, M. Julien and the whole team of the Pérou-Sud archeological project (P.I., D. Lavallée) who have been studying the QLB site since 1995 and provided us with the fossil shells. We thank R. Kaandorp and H. Vonhof for their assistance with isotopic analyses at the Vrije Universiteit, Amsterdam. We are thankful to N. Mitma Garcia for assistance with fieldwork. We thank J. C. Duplessy and O. Kawka for their help. We also thank D. P. Gillikin and an anonymous reviewer for their comments that helped improve this article. This material is based upon work supported by the Pérou-Sud archeological project (MAE, France; P.I., D. Lavallée), the National Geographic Society grant 8122-06 (P.I., M. Carré), by a postdoctoral fellowship of the Joint Institute for the Study of the Atmosphere and Ocean (JISAO) under NOAA cooperative agreement NA17RJ1232, by the U.S. National Science Foundation under grant NSF-ATM-0811382 (P.I., J. P. Sachs), and the U.S. National Oceanic and Atmospheric Administration under grant NOAA-NA08OAR4310685 (P.I., J. P. Sachs). We thank L. Ortlieb and the PNEDC-CONCHAS project who contributed with DIC isotopic analyses. This is ISEM contribution 2011-196.

References

- Addadi, L., and S. Weiner (1992), Control and design principles in biological mineralization, *Angew. Chem. Int. Ed. Engl.*, *31*, 153–169, doi:10.1002/anie.199201531.
- Alvain, S., C. Moulin, Y. Dandonneau, and H. Loisel (2008), Seasonal distribution and succession of dominant phytoplankton groups in the global ocean: A satellite view, *Global Biogeochem. Cycles*, *22*, GB3001, doi:10.1029/2007GB003154.
- Arthur, M. A., D. F. Williams, and D. S. Jones (1983), Seasonal temperature-salinity changes and thermocline development in the mid-Atlantic Bight as recorded by the isotopic composition of bivalves, *Geology*, *11*, 655–659, doi:10.1130/0091-7613(1983)11<655:STCATD>2.0.CO;2.
- Bacastow, R. B., C. D. Keeling, T. J. Lueker, M. Wahlen, and W. G. Mook (1996), The ^{13}C Suess effect in the world surface oceans and its implications for oceanic uptake of CO_2 :

- Analysis of observations at Bermuda, *Global Biogeochem. Cycles*, *10*, 335–346, doi:10.1029/96GB00192.
- Baker, P. A., C. A. Rigsby, G. O. Seltzer, S. C. Fritz, T. K. Lowenstein, N. P. Bacher, and C. Veliz (2001), Tropical climate changes at millennial and orbital timescales on the Bolivian Altiplano, *Nature*, *409*, 698–701, doi:10.1038/35055524.
- Behrenfeld, M. J., R. T. O'Malley, D. A. Siegel, C. R. McClain, J. L. Sarmiento, G. C. Feldman, A. J. Milligan, P. G. Falkowski, R. M. Letelier, and E. S. Boss (2006), Climate-driven trends in contemporary ocean productivity, *Nature*, *444*, 752–755, doi:10.1038/nature05317.
- Bemis, B. E., and D. H. Geary (1996), The usefulness of bivalve stable isotope profiles as environmental indicators: Data from the Eastern Pacific ocean and the southern Caribbean sea, *Palaios*, *11*, 328–339, doi:10.2307/3515243.
- Bétancourt, J. L., C. Latorre, J. A. Rech, J. Quade, and K. A. Rylander (2000), A 22,000-year record of monsoonal precipitation from northern Chile's Atacama desert, *Science*, *289*, 1542–1546.
- Bevelander, G., and P. Benzer (1948), Calcification in marine molluscs, *Biol. Bull.*, *94*, 176–183, doi:10.2307/1538245.
- Böhm, F., M. M. Joachimski, H. Lehnert, G. Morgenroth, W. Kretschmer, J. Vacelet, and W. C. Dullo (1996), Carbon isotope records from extant Caribbean and South Pacific sponges: Evolution of $\delta^{13}\text{C}$ in surface water DIC, *Earth Planet. Sci. Lett.*, *139*, 291–303, doi:10.1016/0012-821X(96)00006-4.
- Bopp, L., P. Monfray, O. Aumont, J.-L. Dufresne, H. L. Treut, G. Madec, L. Terray, and J. C. Orr (2001), Potential impact of climate change on marine export production, *Global Biogeochem. Cycles*, *15*, 81–99, doi:10.1029/1999GB001256.
- Brink, K. H., D. Halpern, A. Huyer, and R. L. Smith (1983), The physical environment of the Peruvian upwelling system, *Prog. Oceanogr.*, *12*, 285–305, doi:10.1016/0079-6611(83)90011-3.
- Broecker, W. S., and E. Maier-Reimer (1992), The influence of air and sea exchange on the carbon isotope distribution in the sea, *Global Biogeochem. Cycles*, *6*, 315–320, doi:10.1029/92GB01672.
- Carré, M., I. Bentaleb, D. Blamart, N. Ogle, F. Cardenas, S. Zevallos, R. M. Kalin, L. Ortlieb, and M. Fontugne (2005a), Stable isotopes and sclerochronology of the bivalve *Mesodesma donacium*: Potential application to Peruvian paleoceanographic reconstructions, *Palaeogeogr. Palaeoclimatol. Palaeoecol.*, *228*, 4–25, doi:10.1016/j.palaeo.2005.03.045.
- Carré, M., I. Bentaleb, M. Fontugne, and D. Lavallée (2005b), Strong El Niño events during the early Holocene: Stable isotope evidence from Peruvian sea-shells, *Holocene*, *15*, 42–47, doi:10.1191/0959683605h1782rp.
- Carré, M., I. Bentaleb, O. Bruguier, E. Ordinola, N. T. Barrett, and M. Fontugne (2006), Calcification rate influence on trace element concentrations in aragonitic bivalve shells: Evidences and mechanisms, *Geochim. Cosmochim. Acta*, *70*, 4906–4920, doi:10.1016/j.gca.2006.07.019.
- Carré, M., L. Klaric, D. Lavallée, M. Julien, I. Bentaleb, M. Fontugne, and O. Kawka (2009), Insights into early Holocene hunter-gatherer mobility on the Peruvian Southern Coast from mollusk gathering seasonality, *J. Archaeol. Sci.*, *36*, 1173–1178, doi:10.1016/j.jas.2009.01.005.
- Carré, M., M. Azzoug, I. Bentaleb, B. M. Chase, M. Fontugne, D. Jackson, M.-P. Ledru, A. Maldonado, J. P. Sachs, and A. J. Schauer (2012), Mid-Holocene mean climate in the south-eastern Pacific and its influence on South America, *Quaternary Int.*, doi:10.1016/j.quaint.2011.02.004, in press.
- Chauvaud, L., J. Thébault, J. Clavier, A. Lorrain, and Ø. Strand (2011), What's hiding behind ontogenetic $\delta^{13}\text{C}$ variations in mollusk shells? New insights from the Great Scallop (*Pecten maximus*), *Estuaries Coasts*, *34*, 211–220, doi:10.1007/s12237-010-9267-4.
- Chávez, F. P., A. Bertrand, R. Guevara-Carrasco, P. Soler, and J. Csirke (2008), The northern Humboldt Current System: Brief history, present status and a view towards the future, *Prog. Oceanogr.*, *79*, 95–105, doi:10.1016/j.pocean.2008.10.012.
- Coale, K. H., et al. (1996), A massive phytoplankton bloom induced by an ecosystem-scale iron fertilization experiment in the equatorial Pacific Ocean, *Nature*, *383*, 495–501, doi:10.1038/383495a0.
- Cole, B. E., and J. E. Cloern (1984), Significance of biomass and light availability to phytoplankton productivity in San Francisco Bay, *Mar. Ecol. Prog. Ser.*, *17*, 15–24, doi:10.3354/meps017015.
- Cox, P. M., R. A. Betts, C. D. Jones, S. A. Spall, and I. J. Totterdell (2000), Acceleration of global warming due to carbon-cycle feedbacks in a coupled climate model, *Nature*, *408*, 184–187, doi:10.1038/35041539.
- Dezileau, L., O. Ulloa, D. Hebbeln, F. Lamy, J.-L. Reyss, and M. Fontugne (2004), Iron control of past productivity in the coastal upwelling system off the Atacama desert, Chile, *Paleoceanography*, *19*, PA3012, doi:10.1029/2004PA001006.
- Duplessy, J.-C., L. Labeyrie, and C. Waelbroeck (2002), Constraints on the ocean oxygen isotopic enrichment between the Last Glacial Maximum and the Holocene: Paleoceanographic implications, *Quat. Sci. Rev.*, *21*, 315–330, doi:10.1016/S0277-3791(01)00107-X.
- Echevin, V., O. Aumont, J. Ledesma, and G. Flores (2008), The seasonal cycle of surface chlorophyll in the Peruvian upwelling system: A modelling study, *Prog. Oceanogr.*, *79*, 167–176, doi:10.1016/j.pocean.2008.10.026.
- Eitel, B., S. Hecht, B. Mächtle, G. Schukraft, A. Kadereit, G. A. Wagner, B. Kromer, I. Unkel, and M. Reindel (2005), Geoarchaeological evidence from desert loess in the Nazca-Palpa region, southern Peru: Palaeoenvironmental changes and their impact on pre-Columbian cultures, *Archaeometry*, *47*, 137–158, doi:10.1111/j.1475-4754.2005.00193.x.
- Elliot, M., P. B. deMenocal, B. K. Linsley, and S. S. Howe (2003), Environmental controls on the stable isotopic composition of *Mercenaria mercenaria*: Potential application to paleoenvironmental studies, *Geochim. Geophys. Geosyst.*, *4*(7), 1056, doi:10.1029/2002GC000425.
- Engel, F. (1957), Early sites on the Peruvian coast, *Southwest. J. Anthropol.*, *13*, 54–68.
- Fontugne, M., M. Carré, I. Bentaleb, M. Julien, and D. Lavallée (2004), Radiocarbon reservoir age variations in the south Peruvian upwelling during the Holocene, *Radiocarbon*, *46*, 531–537.
- Freeman, J. A., and K. M. Wilbur (1948), Carbonic anhydrase in molluscs, *Biol. Bull.*, *94*, 55–59, doi:10.2307/1538209.
- Friedrichs, M. A. M., et al. (2009), Assessing the uncertainties of model estimates of primary productivity in the tropical Pacific Ocean, *J. Mar. Syst.*, *76*, 113–133, doi:10.1016/j.jmarsys.2008.05.010.
- Gillikin, D. P., A. Lorrain, S. Bouillon, P. Willenz, and F. Dehairs (2006a), Stable carbon isotopic composition of *Mytilus edulis* shells: Relation to metabolism, salinity, $\delta^{13}\text{C}_{\text{DIC}}$ and phytoplankton, *Org. Geochem.*, *37*, 1371–1382, doi:10.1016/j.orggeochem.2006.03.008.

- Gillikin, D. P., F. Dehairs, A. Lorrain, D. Steenmans, W. Baeyens, and L. André (2006b), Barium uptake into the shells of the common mussel (*Mytilus edulis*) and the potential for estuarine paleo-chemistry reconstruction, *Geochim. Cosmochim. Acta*, *70*, 395–407, doi:10.1016/j.gca.2005.09.015.
- Gillikin, D. P., A. Lorrain, L. Meng, and F. Dehairs (2007), A large metabolic carbon contribution to the $\delta^{13}\text{C}$ record in marine aragonitic bivalve shells, *Geochim. Cosmochim. Acta*, *71*, 2936–2946, doi:10.1016/j.gca.2007.04.003.
- González, H. E., D. Hebbeln, J. L. Iriarte, and M. Marchant (2004), Downward fluxes of faecal material and microplankton at 2300 m depth in the oceanic area off Coquimbo (30°S), Chile, during 1993–1995, *Deep Sea Res., Part II*, *51*, 2457–2474, doi:10.1016/j.dsr2.2004.07.027.
- Goyet, C., R. Ito Gonçalves, and F. Touratier (2009), Anthropogenic carbon distribution in the eastern South Pacific Ocean, *Biogeosciences*, *6*, 149–156, doi:10.5194/bg-6-149-2009.
- Grossman, E. L., and T.-L. Ku (1986), Oxygen and carbon fractionation in biogenic aragonite: Temperature effect, *Chem. Geol.*, *59*, 59–74, doi:10.1016/0168-9622(86)90057-6.
- Hall, J. G. (1985), The adaptation of enzymes to temperature: Catalytic characterization of glucosephosphate isomerase homologues isolated from *Mytilus edulis* and *Isognomon alatus*, bivalve molluscs inhabiting different thermal environments, *Mol. Biol. Evol.*, *2*, 251–269.
- Holmgren, C. A., J. L. Bétancourt, K. A. Rylander, J. Roque, O. Tovar, H. Zeballos, E. Linares, and J. Quade (2001), Holocene vegetation history from fossil rodent middens near Arequipa, Peru, *Quat. Res.*, *56*, 242–251, doi:10.1006/qres.2001.2262.
- Hutchins, D. A., et al. (2002), Phytoplankton iron limitation in the Humboldt Current and Peru Upwelling, *Limnol. Oceanogr.*, *47*, 997–1011, doi:10.4319/lo.2002.47.4.0997.
- Huyer, A., R. L. Smith, and T. Paluszkiwicz (1987), Coastal upwelling off Peru during normal and El Niño times, 1981–1984, *J. Geophys. Res.*, *92*, 14,297–14,307.
- Ikemoto, N. (1975), Transport and inhibitory Ca^{2+} binding sites on the ATPase enzyme isolated from the sarcoplasmic reticulum, *J. Biol. Chem.*, *250*, 7219–7224.
- Jones, D. S., and W. D. Allmon (1995), Records of upwelling, seasonality and growth in stable-isotope profiles of Pliocene mollusk shells from Florida, *Lethaia*, *28*, 61–74, doi:10.1111/j.1502-3931.1995.tb01593.x.
- Jones, K. B., G. W. L. Hodgins, D. L. Dettman, C. F. T. Andrus, A. Nelson, and M. F. Etayo-Cadavid (2007), Seasonal variations in Peruvian marine reservoir age from pre-bomb *Argopecten purpuratus* shell carbonate, *Radiocarbon*, *49*, 877–888.
- Jones, K. B., G. W. L. Hodgins, M. F. Etayo-Cadavid, and C. F. T. Andrus (2009), Upwelling signals in radiocarbon from early 20th-century Peruvian bay scallop (*Argopecten purpuratus*) shells, *Quat. Res.*, *72*, 452–456, doi:10.1016/j.yqres.2009.07.008.
- Jones, K. B., G. W. L. Hodgins, M. F. Etayo-Cadavid, C. F. T. Andrus, and D. H. Sandweiss (2010), Centuries of marine radiocarbon reservoir age variation within archaeological *Mesodesma donacium* shells from southern Peru, *Radiocarbon*, *52*, 1207–1214.
- Keeling, C. D. (1979), The Suess effect: ^{13}C – ^{14}C interrelations, *Environ. Int.*, *2*, 229–300, doi:10.1016/0160-4120(79)90005-9.
- Keller, N., D. Del Piero, and A. Longinelli (2002), Isotopic composition, growth rate and biological behaviour of *Chamelea gallina* and *Callista chione* from the Gulf of Trieste (Italy), *Mar. Biol. Berlin*, *140*, 9–15, doi:10.1007/s002270100660.
- Killingley, J. S., and W. H. Berger (1979), Stable isotopes in a mollusk shell: Detection of Upwelling events, *Science*, *205*, 186–188, doi:10.1126/science.205.4402.186.
- Klein, R. T., K. C. Lohman, and C. W. Thayer (1996), Sr/Ca and $^{13}\text{C}/^{12}\text{C}$ ratios in skeletal calcite of *Mytilus trossulus*: Covariation with metabolic rate, salinity and carbon isotopic composition of sea water, *Geochim. Cosmochim. Acta*, *60*, 4207–4221, doi:10.1016/S0016-7037(96)00232-3.
- Koutavas, A., and J. P. Sachs (2008), Northern timing of deglaciation in the eastern equatorial Pacific from alkenone paleothermometry, *Paleoceanography*, *23*, PA4205, doi:10.1029/2008PA001593.
- Krantz, D. E., D. F. Williams, and D. S. Jones (1987), Ecological and paleoenvironmental information using stable isotope profiles from living and fossil molluscs, *Palaeogeogr. Palaeoclimatol. Palaeoecol.*, *58*, 249–266, doi:10.1016/0031-0182(87)90064-2.
- Krantz, D. E., A. T. Kronick, and D. F. Williams (1988), A model for interpreting continental-shelf hydrographic processes from the stable isotope and cadmium:calcium profiles of scallop shells, *Palaeogeogr. Palaeoclimatol. Palaeoecol.*, *64*, 123–140, doi:10.1016/0031-0182(88)90002-8.
- Kuentz, A., M.-P. Ledru, and J.-C. Thouret (2012), Environmental changes in the highlands of the western Andean Cordillera, southern Peru, during the Holocene, *Holocene*, doi:10.1177/0959683611409772, in press.
- Lambeck, K., and J. Chappell (2001), Sea level change through the last glacial cycle, *Science*, *292*, 679–686, doi:10.1126/science.1059549.
- Lartaud, F., L. Emmanuel, M. de Rafelis, S. Pouvreau, and M. Renard (2010), Influence of food supply on the $\delta^{13}\text{C}$ signature of mollusc shells: Implications for palaeoenvironmental reconstructions, *Geo-Mar. Lett.*, *30*, 23–34, doi:10.1007/s00367-009-0148-4.
- Lavallée, D., M. Julien, P. Béarez, P. Usselman, M. Fontugne, and A. Bolaños (1999), Pescadores-recolectores arcaicos del extremo-sur Peruano. Excavaciones en la Quebrada de los Burros (Departamento de Tacna). Primeros resultados 1995–1997, *Bull. Inst. Fr. Etude Andines*, *28*, 13–52.
- Liu, H., and A. Warshel (2007), Origin of the temperature dependence of isotope effects in enzymatic reactions: The case of dihydrofolate reductase, *J. Phys. Chem. B*, *111*, 7852–7861, doi:10.1021/jp070938f.
- Lorrain, A., Y.-M. Pualet, L. Chauvaud, R. Dunbar, D. Mucciarone, and M. Fontugne (2004), $\delta^{13}\text{C}$ variation in scallop shells: Increasing metabolic carbon contribution with body size?, *Geochim. Cosmochim. Acta*, *68*, 3509–3519, doi:10.1016/j.gca.2004.01.025.
- Lynch-Stieglitz, J., T. F. Stocker, W. S. Broecker, and R. G. Fairbanks (1995), The influence of air-sea exchange on the isotopic composition of oceanic carbon: Observations and modeling, *Global Biogeochem. Cycles*, *9*, 653–665, doi:10.1029/95GB02574.
- Marin, F., and G. Luquet (2004), Molluscan shell proteins, *C. R. Palevol*, *3*, 469–492, doi:10.1016/j.crpv.2004.07.009.
- Marin, F., G. Luquet, B. Marie, D. Medakovic, and P. S. Gerald (2007), Molluscan shell proteins: Primary structure, origin, and evolution, *Curr. Top. Dev. Biol.*, *80*, 209–276, doi:10.1016/S0070-2153(07)80006-8.
- Martin, J. H., et al. (1994), Testing the iron hypothesis in ecosystems of the equatorial Pacific Ocean, *Nature*, *371*, 123–129, doi:10.1038/371123a0.

- Marxen, J. C., P. E. Witten, D. Finke, O. Reelsen, M. Rezgouai, and W. Becker (2003), A light- and electron-microscopic study of enzymes in the embryonic shell-forming tissue of the freshwater snail, *Biomphalaria glabrata*, *Invertebrate Biol.*, *122*, 313–325, doi:10.1111/j.1744-7410.2003.tb00096.x.
- McConnaughey, T., and D. Gillikin (2008), Carbon isotopes in mollusk shell carbonates, *Geo-Mar. Lett.*, *28*, 287–299, doi:10.1007/s00367-008-0116-4.
- McConnaughey, T. A., J. Burdett, J. F. Whelan, and C. K. Paull (1997), Carbon isotopes in biological carbonates: Respiration and photosynthesis, *Geochim. Cosmochim. Acta*, *61*, 611–622, doi:10.1016/S0016-7037(96)00361-4.
- Mohtadi, M., D. Hebbeln, and M. Marchant (2005), Upwelling and productivity along the Peru-Chile Current derived from faunal and isotopic compositions of planktic foraminifera in surface sediments, *Mar. Geol.*, *216*, 107–126, doi:10.1016/j.margeo.2005.01.008.
- Mook, W. G. (1971), Paleotemperatures and chlorinities from stable carbon and oxygen isotopes in shell carbonate, *Palaeogeogr. Palaeoclimatol. Palaeoecol.*, *9*, 245–263, doi:10.1016/0031-0182(71)90002-2.
- Mook, W. G., and J. C. Vogel (1968), Isotopic equilibrium between shells and their environment, *Science*, *159*, 874–875, doi:10.1126/science.159.3817.874.
- Northrop, D. B. (1981), The expression of isotope effects on enzyme-catalyzed reactions, *Annu. Rev. Biochem.*, *50*, 103–131, doi:10.1146/annurev.bi.50.070181.000535.
- Ochoa, N., M. H. Taylor, S. Purga, and E. Ramos (2010), Intra- and interannual variability of nearshore phytoplankton biovolume and community changes in the northern Humboldt Current system, *J. Plankton Res.*, *32*, 843–855, doi:10.1093/plankt/fbq022.
- Ortlieb, L., G. Vargas, and J.-F. Saliège (2011), Marine radiocarbon reservoir effect along the northern Chile-southern Peru coast (14–24°S) throughout the Holocene, *Quat. Res.*, *75*, 91–103, doi:10.1016/j.yqres.2010.07.018.
- Pick, U., and S. J. Karlsh (1982), Regulation of the conformation transition in the Ca-ATPase from sarcoplasmic reticulum by pH, temperature, and calcium ions, *J. Biol. Chem.*, *257*, 6120–6126.
- Placzek, C., J. Quade, and J. L. Bétancourt (2001), Holocene lake-level fluctuations of lake Aricota, southern Peru, *Quat. Res.*, *56*, 181–190, doi:10.1006/qres.2001.2263.
- Quay, P. B., B. Tilbrook, and C. S. Wong (1992), Oceanic uptake of fossil fuel CO₂: Carbon-13 evidence, *Science*, *256*, 74–79, doi:10.1126/science.256.5053.74.
- Quay, P., R. Sonnerup, T. Westby, J. Stutsman, and A. McNichol (2003), Changes in the ¹³C/¹²C of dissolved inorganic carbon in the ocean as a tracer of anthropogenic CO₂ uptake, *Global Biogeochem. Cycles*, *17*(1), 1004, doi:10.1029/2001GB001817.
- Rech, J. A., J. S. Pigati, J. Quade, and J. L. Bétancourt (2003), Re-evaluation of mid-Holocene deposits at Quebrada Puripica, northern Chile, *Palaeogeogr. Palaeoclimatol. Palaeoecol.*, *194*, 207–222, doi:10.1016/S0031-0182(03)00278-5.
- Rein, B., A. Lückge, L. Reinhardt, F. Sirocko, A. Wolf, and W.-C. Dullo (2005), El Niño variability off Peru during the last 20,000 years, *Paleoceanography*, *20*, PA4003, doi:10.1029/2004PA001099.
- Romanek, C. S., and E. L. Grossman (1989), Stable isotope profiles of *Tridacna maxima* as environmental indicators, *Palaios*, *4*, 402–413, doi:10.2307/3514585.
- Romanek, C. S., E. L. Grossman, and J. W. Morse (1992), Carbon isotopic fractionation in synthetic aragonite and calcite: Effects of temperature and precipitation rate, *Geochim. Cosmochim. Acta*, *56*, 419–430, doi:10.1016/0016-7037(92)90142-6.
- Schowen, K. B., and R. L. Schowen (1981), The use of isotope effects to elucidate enzyme mechanisms, *BioScience*, *31*, 826–831, doi:10.2307/1308680.
- Somero, G. N. (1969), Enzymatic mechanisms of temperature compensation: Immediate and evolutionary effects of temperature on enzymes of aquatic poikilotherms, *Am. Nat.*, *103*, 517–530, doi:10.1086/282618.
- Stecher, H. A., III, D. E. Krantz, C. J. Lord III, G. W. Luther III, and K. W. Bock (1996), Profiles of strontium and barium in *Mercenaria mercenaria* and *Spisula solidissima* shells, *Geochim. Cosmochim. Acta*, *60*, 3445–3456, doi:10.1016/0016-7037(96)00179-2.
- Steinacher, M., et al. (2010), Projected 21st century decrease in marine productivity: A multi-model analysis, *Biogeosciences*, *7*, 979–1005, doi:10.5194/bg-7-979-2010.
- Strub, P. T., J. M. Mesias, V. Montecino, J. Rutllant, and S. Salinas (1998), Coastal ocean circulation off western South America, in *The Global Coastal Ocean. Regional Studies and Syntheses*, edited by A. R. Robinson and K. H. Brink, pp. 273–315, Wiley, New York.
- Suzuki, M., K. Saruwatari, T. Kogure, Y. Yamamoto, T. Nishimura, T. Kato, and H. Nagasawa (2009), An acidic matrix protein, Pif, is a key macromolecule for nacre formation, *Science*, *325*, 1388–1390, doi:10.1126/science.1173793.
- Tanaka, N., M. C. Monaghan, and D. M. Rye (1986), Contribution of metabolic carbon to mollusc and barnacle shell carbonate, *Nature*, *320*, 520–523, doi:10.1038/320520a0.
- Taylor, M. H., M. Wolff, J. Mendo, and C. Yamashiro (2008), Changes in trophic flow structure of Independence Bay (Peru) over an ENSO cycle, *Prog. Oceanogr.*, *79*, 336–351, doi:10.1016/j.pocean.2008.10.006.
- Thébault, J., L. Chauvaud, S. L’Helguen, J. Clavier, A. Barats, S. Jacquet, C. Pécheyran, and D. Amouroux (2009), Barium and molybdenum records in bivalve shells: Geochemical proxies for phytoplankton dynamics in coastal environments?, *Limnol. Oceanogr.*, *54*, 1002–1014, doi:10.4319/lo.2009.54.3.1002.
- Thomas, A. C., F. Huang, P. T. Strub, and C. James (1994), Comparison of the seasonal and interannual variability of phytoplankton pigment concentrations in the Peru and California Current systems, *J. Geophys. Res.*, *99*, 7355–7370, doi:10.1029/93JC02146.
- Vander Putten, E., F. Dehairs, E. Keppens, and W. Baeyens (2000), High resolution distribution of trace elements in the calcite shell layer of modern *Mytilus edulis*: Environmental and biological controls, *Geochim. Cosmochim. Acta*, *64*, 997–1011, doi:10.1016/S0016-7037(99)00380-4.
- Verkouteren, R. M. (1999), Preparation, characterization, and value assignment of carbon dioxide isotopic reference materials: RMs 8562, 8563, and 8564, *Anal. Chem.*, *71*, 4740–4746, doi:10.1021/ac990233c.
- Watabe, N., and K. M. Wilbur (1960), Influence of the organic matrix on crystal type in molluscs, *Nature*, *188*, 334, doi:10.1038/188334a0.
- Wheeler, A. P., J. W. George, and C. A. Evans (1981), Control of calcium carbonate nucleation and crystal growth by soluble matrix of oyster shell, *Science*, *212*, 1397–1398, doi:10.1126/science.212.4501.1397.
- Wolfenden, R., M. Snider, C. Ridgway, and B. Miller (1999), The temperature dependence of enzyme rate enhancements, *J. Am. Chem. Soc.*, *121*, 7419–7420, doi:10.1021/ja991280p.